INORGANIC CHEMISTRY FRONTIERS

RESEARCH ARTICLE

View Article Online
View Journal | View Issue

Check for updates

Cite this: *Inorg. Chem. Front.*, 2024, **11**, 3263

Stepwise synthesis of heterotrimetallic $Fe^{II}/Pd^{II}/Au^{I}$ coordination cages†

Noga Eren, Farzaneh Fadaei-Tirani and Kay Severin *

Received 4th February 2024,
Accepted 24th April 2024

DOI: 10.1039/d4qi00340c

rsc.li/frontiers-inorganic

The synthesis of heterotrimetallic molecular cages is reported. The assemblies contain three types of coordination compounds: Fe^{II} clathrochelate complexes, Au^{I}_3(pyrazolate)$_3$ complexes, and $[Pd^{II}(pyridine)_4]^{2+}$ complexes. The cages were obtained in a stepwise fashion. A nanometer-sized metalloligand with three terminal 3-pyridyl donor groups was prepared by connection of three Fe^{II} clathrochelate complexes *via* a central Au_3(pyrazolate)$_3$ complex. A related strategy was employed for the synthesis of a ditopic N-donor ligand with two functionalized Fe^{II} clathrochelate complexes. Combining the tritopic ligand with $[Pd(CH_3CN)_4](BF_4)_2$ resulted in the clean formation of a spherical $Pd^{II}_6Fe^{II}_{24}Au^{I}_{24}$ coordination cage with a diameter of ~4.1 nm and a molecular weight of 21 kDa. The ditopic metalloligand was used for the construction of a $Pd^{II}_2Fe^{II}_8Au^{I}_{12}$ cage.

Open Access Article. Published on 29 April 2024. Downloaded on 1/30/2026 12:38:18 AM.
This article is licensed under a Creative Commons Attribution 3.0 Unported Licence.

Introduction

Heterometallic coordination cages are attractive synthetic targets because the presence of different metal centers within one assembly can potentially lead to interesting new functions and properties.[1] For the preparation of heterometallic cages, two main strategies have been explored. The first strategy relies on the use of polydentate ligands with distinct binding sites for the respective metal ions. A chemoselective complexation can be achieved by presenting different donor groups (*e.g.*, hard and soft donors for hard and soft metal ions), or by exploiting the preference of a metal ion for a certain coordination geometry.[2] The second strategy circumvents selectivity problems by introducing different metal ions in a step-wise fashion under kinetic control.[3] Metalloligands play an important role in this context. Metalloligands are coordination compounds with donor groups in their ligand periphery.[4] Due to the inert character of metalloligands, reactions with other metal ions can be performed without ligand scrambling.

The above-mentioned strategies have been used with great success for the construction of heterobimetallic coordination cages.[1–4] However, the synthesis of cages containing three different metal ions is still challenging, and only a few examples have been reported in the literature.[1,4,5]

Below, we describe the synthesis of a heterotrimetallic $Pd^{II}_6Fe^{II}_{24}Au^{I}_{24}$ coordination cage. This cage was obtained by an Fe^{2+}-templated polycondensation reaction, followed by regioselective complexation with Au^{+}, and a final self-assembly step with Pd^{2+} (Scheme 1). A related strategy was used to prepare a cage with two Pd^{2+} ions, 8 Fe^{2+} ions, and 12 Au^{+} ions.

Results and discussion

Recently, we reported the synthesis of molecular cages containing trinuclear Au^{I}_3(pyrazolate)$_3$ complexes.[6] The cages were obtained by connection of pre-formed gold complexes *via* dynamic covalent imine chemistry. The incorporation of Au^{I}_3

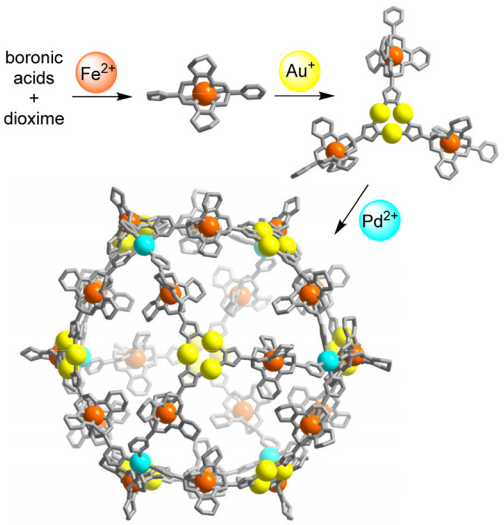

Scheme 1 Stepwise synthesis of a coordination cage containing 6 Pd^{2+} ions, 24 Fe^{2+} ions, and 24 Au^{+} ions.

Institut des Sciences et Ingénierie Chimiques, École Polytechnique Fédérale de Lausanne (EPFL), 1015 Lausanne, Switzerland. E-mail: kay.severin@epfl.ch

†Electronic supplementary information (ESI) available: Synthetic procedures and experimental details. CCDC 2325913–2325915. For ESI and crystallographic data in CIF or other electronic format see DOI: https://doi.org/10.1039/d4qi00340c

Open Access Article. Published on 29 April 2024. Downloaded on 1/30/2026 12:38:18 AM.
This article is licensed under a Creative Commons Attribution 3.0 Unported Licence.

(pyrazolate)$_3$ trimers into cages was motivated by the properties of these complexes: as highly π-basic compounds, they tend to form aggregates with π- or Lewis acids.[7] Indeed, prismatic cages with two Au^I_3(pyrazolate)$_3$ faces were found to encapsulate π-acidic aromatic compounds.[6] Furthermore, we observed strong fullerene binding by a tetrahedral cage containing four Au^I_3(pyrazolate)$_3$ complexes.[6]

For the present study, we explored the incorporation of Au^I_3(pyrazolate)$_3$ trimers into heterometallic coordination cages. One challenge in building more complex nanostructures with Au^I_3(pyrazolate)$_3$ complexes is the tendency of these trimers to form intermolecular Au···Au interactions. As a result, Au^I_3(pyrazolate)$_3$ complexes often display low solubility.[7,8] We hypothesized that solubility issues could be addressed by fusion of Au^I_3(pyrazolate)$_3$ complexes to boronate ester-capped clathrochelate complexes.[4c,9] The three-dimensional structure of the latter disfavors stacking interactions, and molecular nanostructures based on clathrochelates often display good solubility in organic solvents.[4c,10]

In order to connect clathrochelates with Au^I_3(pyrazolate)$_3$ complexes, we first synthesized the Fe^{II} clathrochelate **1** (Scheme 2). This compound was obtained by a metal-templated polycondensation reaction involving four commercially available compounds: (1*H*-pyrazol-4-yl)boronic acid, 3-pyridylboronic acid, nioxime, and $FeCl_2$. Due to the presence of two different boronic acids, symmetric clathrochelates with identical capping groups are obtained along with target **1**. Chromatographic purification gave complex **1** in 26% yield.

The solid-state structure of **1** was analyzed by single-crystal X-ray diffraction (XRD). The central Fe^{II} center in **1** displays a distorted trigonal prismatic coordination environment (Fig. 1), which is typical for such complexes.[9] The Fe–N bond lengths are within the expected range (1.902(2)–1.913(2) Å).

Next, we have combined complex **1** with AuCl(SMe$_2$) and NEt$_3$ (Scheme 3). Based on literature reports,[11] we expected a regioselective complexation of Au^I to the pyrazole part of **1**. Indeed, we were able to isolate the desired Au_3(pyrazolate)$_3$ complex **2** in high yield (87%).

Complex **2** was found to be well soluble in dichloromethane and chloroform, but poorly soluble in acetonitrile or diethyl ether. The apparent C_3 symmetry of **2** was reflected in the NMR spectra, which showed one set of signals for the three

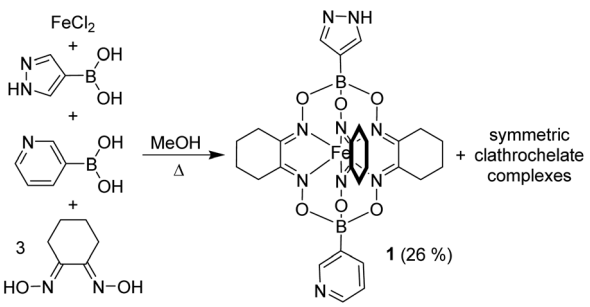

Scheme 2 Synthesis of complex **1**.

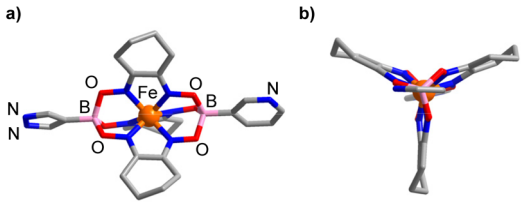

Fig. 1 Molecular structure of complex **1** in the crystal with a view from the side (a) and along the B···B axis (b). Hydrogen atoms and co-crystallized solvent molecules are not shown.

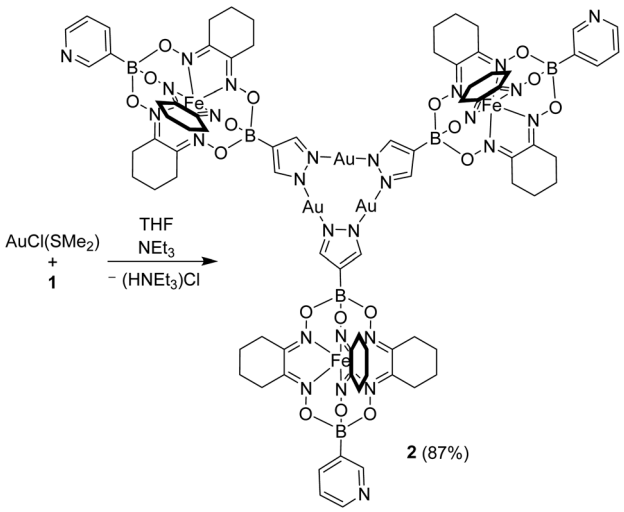

Scheme 3 Synthesis of complex **2**.

clathrochelate groups. The formation of a trimeric structure could be confirmed by high-resolution mass spectrometry.[12]

An XRD analysis of complex **2** confirmed that three clathrochelate complexes are connected *via* the pyrazolate N-atoms to three Au^+ ions (Fig. 2a). In the solid state, two complexes form a closely packed dimer, with the Au^I_3(pyrazolate)$_3$ complexes being positioned on top of each other (Fig. 2b). The arrangement seems to imply intermolecular aurophilic interactions. However, the shortest Au···Au distance is 3.8250(6) Å. This value is significantly larger than what is found for the solid-state structures of other Au_3(pyrazolate)$_3$ complexes, with typical Au···Au contacts in the range of 3.3 Å.[7] Possibly, the bulky clathrochelates in **2** hamper a closer packing of the Au^I_3(pyrazolate)$_3$ complexes. Another noteworthy feature of crystalline **2** is the non-planar arrangement of the three pyrazolate heterocycles. As a result, the plane defined by the three Fe^{2+} ions is inclined with respect to the plane defined by the three Au^+ ions (Fig. 2c).

During previous studies, we had noted that Au^I_3(pyrazolate)$_3$ complexes display a high kinetic inertness. This characteristic suggested that it might be possible to prepare low-symmetry complexes with different pyrazolate ligands. In order to investigate this point, we have examined the reaction between AuCl(SMe$_2$) (3 eq.) and a mixture of complex **1** (2 eq.) and 3,5-

This journal is © the Partner Organisations 2024

Open Access Article. Published on 29 April 2024. Downloaded on 1/30/2026 12:38:18 AM.
This article is licensed under a Creative Commons Attribution 3.0 Unported Licence.

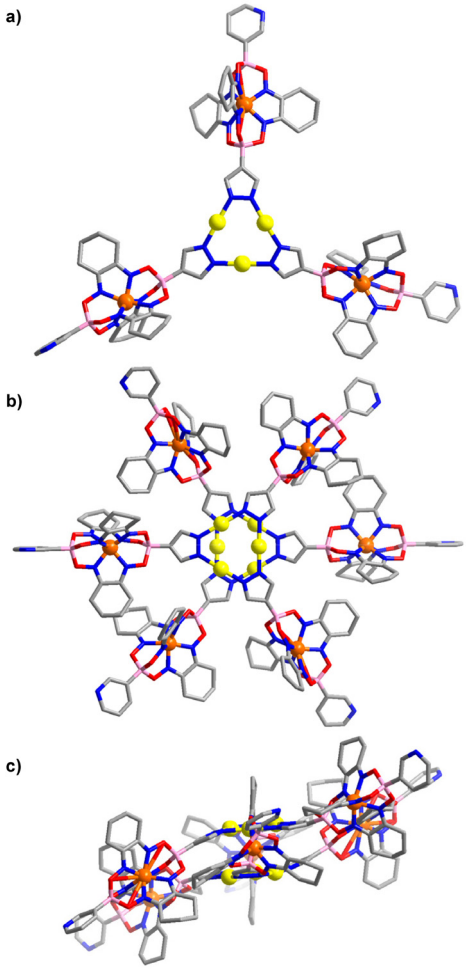

Fig. 2 Molecular structure of complex **2** in the crystal (a), and two different views of the relative arrangement of two adjacent complexes (b and c). Hydrogen atoms are not shown. Color coding: C (gray), N (blue), O (red), B (pink), Au (yellow).

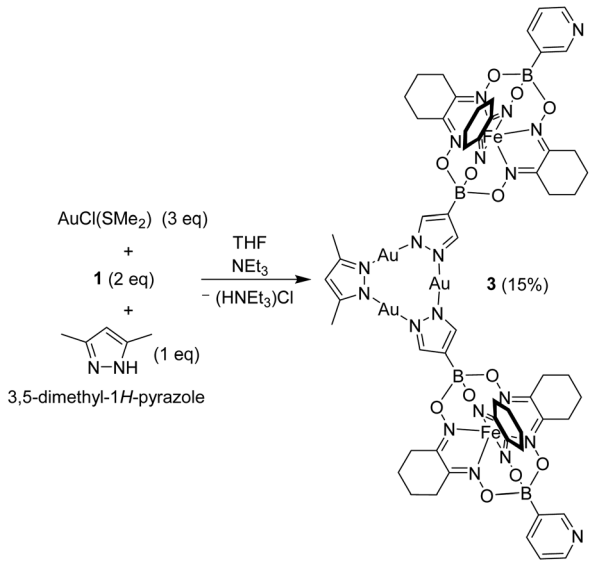

Scheme 4 Synthesis of complex **3**.

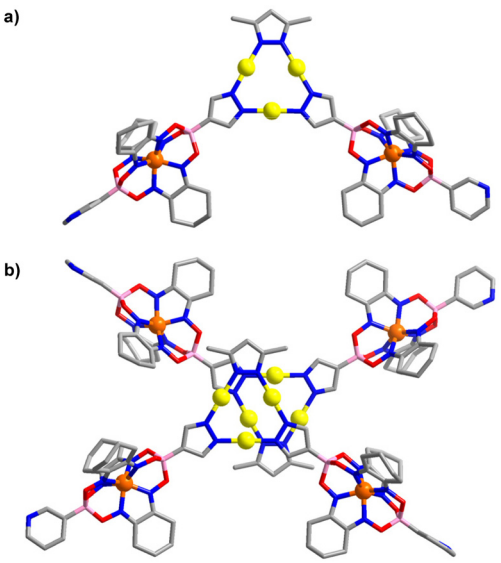

Fig. 3 Molecular structure of complex **3** in the crystal (a), and the relative arrangement of two adjacent complexes (b). Hydrogen atoms are not shown. Color coding: C (gray), N (blue), O (red), B (pink), Au (yellow).

dimethyl-1*H*-pyrazole (1 eq.) in the presence of NEt_3 (Scheme 4). As expected, a mixture of products was obtained, including the symmetric trimer **2** (detected by mass spectrometry). Chromatographic purification gave the desired ditopic pyridyl ligand **3** in 15% yield.

Complex **3** displays similar solubility properties as **2**: it is soluble in dichloromethane and chloroform, but poorly soluble in acetonitrile. The NMR spectra were in line with the depicted structure, with one set of signals for the two clathrochelate groups, and one set of signals for the dimethylpyrazolate ligand. To the best of our knowledge, complex **3** represents the first example of a Au^{I}_3(pyrazolate)$_3$ complex with two different pyrazolate ligands.[13]

The molecular structure of complex **3** in the crystal is depicted in Fig. 3. As in the case of **2**, one can observe a stacked arrangement of the Au^{I}_3(pyrazolate)$_3$ units of two adjacent complexes. Two close Au···Au contacts are observed (3.35(1) Å), indicating the presence of aurophilic interactions. Despite the presence of Au···Au interactions, complex **3** was not luminescent in the solid state.

With the heterometallic ligands **2** and **3** in hand, we next studied reactions with Pd^{2+}. Based on the geometry of ligand **2** (C_3 symmetric ligand with terminal 3-pyridyl groups), we expected that a $[Pd_6L_8]^{12+}$-type cage might form.[3i,10d,14] When a solution of metalloligands **2** (4 eq.) and $[Pd(CH_3CN)_4](BF_4)_2$ in DMSO-d_6 was heated to 60 °C for 15 h, a defined assembly with high apparent symmetry was obtained, as indicated by the NMR spectra (^{1}H NMR and DOSY). The high-resolution mass spectrum confirmed that a $[Pd_6L_8]^{12+}$-type cage (**4**) had formed (Scheme 5 and Fig. 4).

Open Access Article. Published on 29 April 2024. Downloaded on 1/30/2026 12:38:18 AM.
This article is licensed under a Creative Commons Attribution 3.0 Unported Licence.

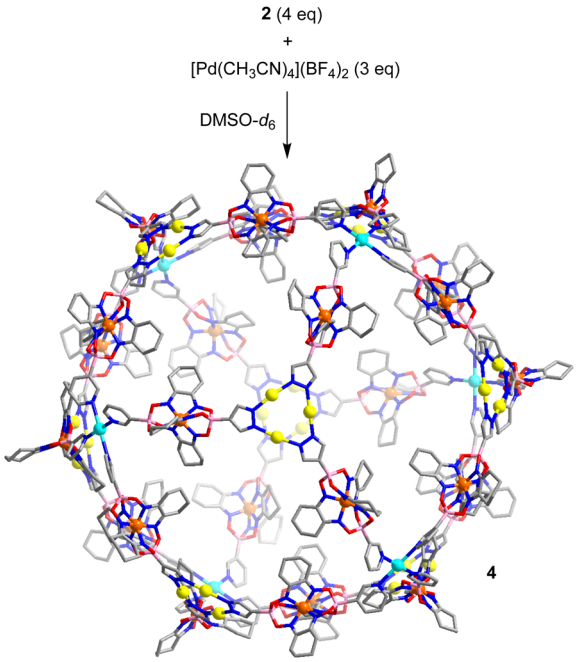

Scheme 5 Synthesis of cage **4**. The structure of the product is based on molecular modeling. Color coding: C (gray), N (blue), O (red), B (pink), Au (yellow), Pd (cyan).

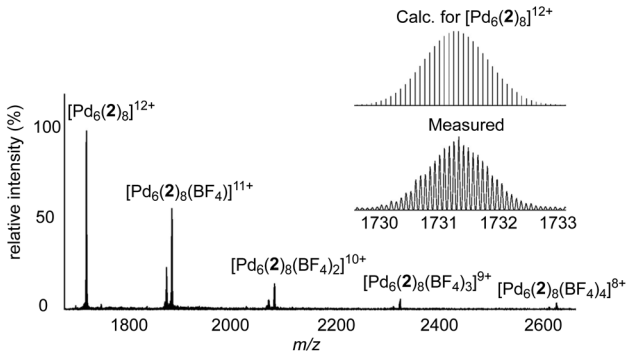

Fig. 4 High-resolution ESI mass spectrum of cage **4**.

The cationic cage **4** has a molecular weight of 21 kDa. This value is in the range found for small proteins. For example, myoglobin has a molecular weight of 17 kDa.[15] Attempts to grow single crystals of **4** were not successful. Molecular modelling showed that cage **4** has a diameter of approximately 4.1 nm.[16] This value is in agreement with the solvodynamic diameter of cage **4**, which was deduced from the DOSY spectrum (4.3 nm).[17]

The ditopic N-donor ligand **3** is able to adopt a conformation with a parallel orientation of the coordinate vectors. As a result, it should be well suited to form $[M_2L_4]^{4+}$-type cages.[18] Thermal equilibration of a mixture of ligand **3** (2 eq.) and $[Pd(CH_3CN)_4](BF_4)_2$ (1 eq.) in DMSO-d_6 resulted indeed in the formation of a dinuclear Pd^{II} complex with four bridging metalloligands (cage **5**, Scheme 6). Cage **5** was characterized by NMR

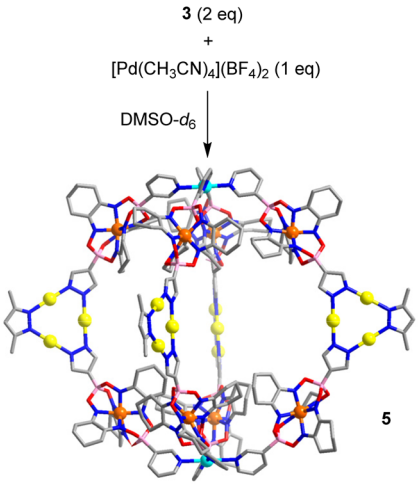

Scheme 6 Synthesis of cage **5**. The structure of the product is based on molecular modeling. Color coding: C (gray), N (blue), O (red), B (pink), Au (yellow), Pd (cyan).

spectroscopy (^{1}H NMR, DOSY) and mass spectrometry (see the ESI, Fig. S17†). According to the results of molecular modelling, the Pd^{2+} ions in cage **5** are ~2.4 nm apart from each other. The width of the assembly, as defined by the maximum C···C distance, is ~3.5 nm.

Conclusions

We have reported the synthesis of heterometallic cages containing three types of coordination compounds: Fe^{II} clathrochelate complexes, Au^{I}_3(pyrazolate)$_3$ complexes, and $[Pd^{II}(pyridine)_4]^{2+}$ complexes. The cages were obtained in a stepwise fashion. First, we prepared di- and tritopic metalloligands by connecting two or three functionalized Fe^{II} clathrochelates *via* Au^{I}_3(pyrazolate)$_3$ complexes. The tritopic ligand (**2**) was then combined with $[Pd(CH_3CN)_4](BF_4)_2$ to give a spherical $Pd^{II}_6Fe^{II}_{24}Au^{I}_{24}$ coordination cage (**4**). With a weight of 21 kDa and a diameter of ~4.1 nm, this complex is one of the largest $[Pd_6L_8]^{12+}$-type cages reported to date. The ditopic ligand (**3**) was used to construct a $Pd^{II}_2Fe^{II}_8Au^{I}_{12}$ coordination cage (**5**).

In previous work, we had shown that functionalized Fe^{II} clathrochelate complexes are well-suited to build large and well-soluble metallosupramolecular structures.[4c] With the present work, we demonstrate that clathrochelate-based metalloligands can be combined with Au^{I}_3(pyrazolate)$_3$ complexes. The inert character of the Au^{I} trimers is important because it enables a final metal-based self-assembly step (here with Pd^{2+}) without ligand scrambling. Furthermore, it is possible to prepare heteroleptic Au^{I}_3(pyrazolate)$_3$ complexes containing different pyrazolate ligands. As a proof-of-concept, we have prepared the mixed-ligand complex **3** using a statistical synthesis followed by chromatographic separation. Other low-symmetry ligands based on Au^{I}_3(pyrazolate)$_3$ trimers can likely be accessed in a similar fashion. In our opinion, Au^{I}_3(pyrazolate)$_3$-

 This journal is © the Partner Organisations 2024

based metalloligands have great potential as building blocks in supramolecular chemistry.

Author contributions

N. E. and K. S. initiated the study, N. E. performed the experiments and analyzed the data, F. F.-T. collected and processed the X-ray data, and N. E. and K. S. co-wrote the manuscript. All authors discussed the results and commented on the manuscript.

Conflicts of interest

There are no conflicts to declare.

Acknowledgements

The work was supported by the École Polytechnique Fédérale de Lausanne (EPFL). We thank Dr Ru-Jin Li for his help with the syntheses.

References

1 For review articles, see: (*a*) L. K. Moree, L. A. V. Faulkner and J. D. Crowley, Heterometallic cages: synthesis and applications, *Chem. Soc. Rev.*, 2024, **53**, 25–46; (*b*) M. Hardy and A. Lützen, Better Together: Functional Heterobimetallic Macrocyclic and Cage-like Assemblies, *Chem. – Eur. J.*, 2020, **26**, 13332–13346; (*c*) W.-X. Gao, H.-N. Zhang and G.-X. Jin, Supramolecular catalysis based on discrete heterometallic coordination-driven metallacycles and metallacages, *Coord. Chem. Rev.*, 2019, **386**, 69–84; (*d*) Y.-Y. Zhang, W.-X. Gao, L. Lin and G.-X. Jin, Recent advances in the construction and applications of heterometallic macrocycles and cages, *Coord. Chem. Rev.*, 2017, **344**, 323–344; (*e*) H. Li, Z.-J. Yao, D. Liu and G.-X. Jin, Multi-component coordination-driven self-assembly toward heterometallic macrocycles and cages, *Coord. Chem. Rev.*, 2015, **293–294**, 139–157.

2 For examples, see: (*a*) J. P. Carpenter, T. K. Ronson, F. J. Rizzuto, T. Héliot, P. Grice and J. R. Nitschke, Incorporation of a Phosphino(pyridine) Subcomponent Enables the Formation of Cages with Homobimetallic and Heterobimetallic Vertices, *J. Am. Chem. Soc.*, 2022, **144**, 8467–8473; (*b*) Y. Yang, Y. Wu, J.-H. Jia, X.-Y. Zheng, Q. Zhang, K.-C. Xiong, Z.-M. Zhang and Q.-M. Wang, Enantiopure Magnetic Heterometallic Coordination Cubic Cages $[M^{II}{}_8Cu^{II}{}_6]$ (M = Ni, Co), *Cryst. Growth Des.*, 2018, **18**, 4555–4561; (*c*) G. Liu, M. Zeller, K. Su, J. Pang, Z. Ju, D. Yuan and M. Hong, Controlled Orthogonal Self-Assembly of Heterometal-Decorated Coordination Cages, *Chem. – Eur. J.*, 2016, **22**, 17345–17350; (*d*) H. Li, Y.-F. Han, Y.-J. Lin, Z.-W. Guo and G.-X. Jin, Stepwise Construction of Discrete Heterometallic Coordination Cages Based on Self-Sorting Strategy, *J. Am. Chem. Soc.*, 2014, **136**, 2982–2985; (*e*) Y. Sakata, S. Hiraoka and M. Shionoya, Site-Selective Ligand Exchange on a Heteroleptic Ti^{IV} Complex Towards Stepwise Multicomponent Self-Assembly, *Chem. – Eur. J.*, 2010, **16**, 3318–3325; (*f*) S. Hiraoka, Y. Sakata and M. Shionoya, Ti(IV)-Centered Dynamic Interconversion between Pd(II), Ti(IV)-Containing Ring and Cage Molecules, *J. Am. Chem. Soc.*, 2008, **130**, 10058–10059.

3 For examples, see: (*a*) A. C. Pearcy, L. S. Lisboa, D. Preston, N. B. Page, T. Lawrence, L. J. Wright, C. G. Hartinger and J. D. Crowley, Exploiting reduced-symmetry ligands with pyridyl and imidazole donors to construct a second-generation stimuli-responsive heterobimetallic $[PdPtL_4]^{4+}$ cage, *Chem. Sci.*, 2023, **14**, 8615–8623; (*b*) Q.-Y. Zhu, L.-P. Zhou, L.-X. Cai, S.-J. Hu, X.-Z. Li and Q.-F. Sun, Stereocontrolled Self-Assembly of Ln(III)–Pt(II) Heterometallic Cages with Temperature-Dependent Luminescence, *Inorg. Chem.*, 2022, **61**, 16814–16821; (*c*) M. Hardy, M. Engeser and A. Lützen, A heterobimetallic tetrahedron from a linear platinum(II)-bis (acetylide) metalloligands, *Beilstein J. Org. Chem.*, 2020, **16**, 2701–2708; (*d*) L. S. Lisboa, J. A. Findlay, L. J. Wright, C. G. Hartinger and J. D. Crowley, A Reduced-Symmetry Heterobimetallic $[PdPtL_4]^{4+}$ Cage: Assembly, Guest Binding, and Stimulus-Induced Switching, *Angew. Chem., Int. Ed.*, 2020, **59**, 11101–11107; (*e*) A. A. Adeyemo and P. S. Mukherjee, Coordination-driven self-assembly of discrete Ru_6–Pt_6 prismatic cages, *Beilstein J. Org. Chem.*, 2018, **14**, 2242–2249; (*f*) A. J. Metherell and M. D. Ward, Imposing control on self-assembly: rational design and synthesis of a mixed-metal, mixed-ligand coordination cage containing four types of component, *Chem. Sci.*, 2016, **7**, 910–915; (*g*) C. Heindl, E. V. Peresypkina, A. V. Virovets, W. Kremer and M. Scheer, Giant Rugby Ball $[\{Cp^{Bn}Fe(\eta^5\text{-}P_5)\}_{24}Cu_{96}Br_{96}]$ Derived from Pentaphosphaferrocene and $CuBr_2$, *J. Am. Chem. Soc.*, 2015, **137**, 10938–10941; (*h*) S. Sanz, H. M. O'Connor, E. M. Pineda, K. S. Pedersen, G. S. Nichol, O. Mønsted, H. Weihe, S. Piligkos, E. J. L. McInnes, P. J. Lusby and E. K. Brechin, $[Cr^{III}{}_8M^{II}{}_6]^{12+}$ Coordination Cubes (M^{II} = Cu, Co), *Angew. Chem., Int. Ed.*, 2015, **54**, 6761–6764; (*i*) K. Li, L.-Y. Zhang, C. Yan, S.-C. Wei, M. Pan, L. Zhang and C.-Y. Su, Stepwise Assembly of $Pd_6(RuL_3)_8$ Nanoscale Rhombododecahedral Metal–Organic Cages via Metalloligand Strategy for Guest Trapping and Protection, *J. Am. Chem. Soc.*, 2014, **136**, 4456–4459; (*j*) W. J. Ramsay, T. K. Ronson, J. K. Clegg and J. R. Nitschke, Bidirectional Regulation of Halide Binding in a Heterometallic Supramolecular Cube, *Angew. Chem., Int. Ed.*, 2013, **52**, 13439–13443.

4 For review articles, see: (*a*) F. Li and L. F. Lindoy, Complementarity and Preorganisation in the Assembly of Heterometallic–Organic Cages via the Metalloligand Approach—Recent Advances, *Chemistry*, 2021, **4**, 1439–1456; (*b*) F. Li and L. F. Lindoy, Metalloligand Strategies for Assembling Heteronuclear Nanocages – Recent Developments, *Aust. J. Chem.*, 2019, **72**, 731–741;

Open Access Article. Published on 29 April 2024. Downloaded on 1/30/2026 12:38:18 AM. This article is licensed under a Creative Commons Attribution 3.0 Unported Licence.

Open Access Article. Published on 29 April 2024. Downloaded on 1/30/2026 12:38:18 AM. This article is licensed under a Creative Commons Attribution 3.0 Unported Licence.

(*c*) S. M. Jansze and K. Severin, Clathrochelate Metalloligands in Supramolecular Chemistry and Materials Science, *Acc. Chem. Res.*, 2018, **51**, 2139–2147; (*d*) J. Gil-Rubio and J. Vicente, *Chem. – Eur. J.*, 2018, **24**, 32–46; (*e*) L. Li, D. J. Fanna, N. D. Shepherd and L. F. Lindoy, Constructing coordination nanocages: the metalloligand approach, *J. Inclusion Phenom. Macrocyclic Chem.*, 2015, **82**, 3–12; (*f*) E. Iengo, P. Cavigli, D. Milano and P. Tecilla, Metal mediated self-assembled porphyrin metallacycles: Synthesis and multipurpose applications, *Inorg. Chim. Acta*, 2014, **417**, 59–78; (*g*) S. Durot, J. Taesch and V. Heitz, Multiporphyrinic Cages: Architectures and Functions, *Chem. Rev.*, 2014, **114**, 8542–8578; (*h*) G. Kumar and R. Gupta, Molecularly designed architectures – the metalloligand way, *Chem. Soc. Rev.*, 2013, **42**, 9403–9453; (*i*) M. C. Das, S. Xiang, Z. Zhang and B. Chen, Functional Mixed Metal–Organic Frameworks with Metalloligands, *Angew. Chem., Int. Ed.*, 2011, **50**, 10510–10520; (*j*) E. C. Constable, Expanded ligands—An assembly principle for supramolecular chemistry, *Coord. Chem. Rev.*, 2008, **252**, 842–855.

5 For examples, see: (*a*) H. Ube, K. Endo, H. Sato and M. Shionoya, Synthesis of Hetero-multinuclear Metal Complexes by Site-Selective Redox Switching and Transmetalation on a Homo-multinuclear Complex, *J. Am. Chem. Soc.*, 2019, **141**, 10384–10389; (*b*) J. Ferrando-Soria, A. Fernandez, D. Asthana, S. Nawaz, I. Vitorica-Yrezabal, G. F. S. Whitehead, C. A. Muryn, F. Tuna, G. A. Timco, N. D. Burton and R. E. P. Winpenny, A [13]rotaxane assembled via a palladium molecular capsule, *Nat. Commun.*, 2019, **10**, 3720; (*c*) H. Brake, E. Peresypkina, C. Heindl, A. V. Virovets, W. Kremer and M. Scheer, From nano-balls to nano-bowls, *Chem. Sci.*, 2019, **10**, 2940–2944; (*d*) J. Jiao, C. Tan, Z. Li, Y. Liu, X. Han and Y. Cui, Design and Assembly of Chiral Coordination Cages for Asymmetric Sequential Reactions, *J. Am. Chem. Soc.*, 2018, **140**, 2251–2259; (*e*) M. Chen, J. Wang, S. Chakraborty, D. Liu, Z. Jiang, Q. Liu, J. Yan, H. Zhong, G. R. Newcome and P. Wang, Metallosupramolecular 3D assembly of dimetallic $Zn_4[RuL_2]_2$ and trimetallic $Fe_2Zn_2[RuL_2]_2$, *Chem. Commun.*, 2017, **53**, 11087–11090; (*f*) K. Su, F. Jiang, J. Qian, L. Chen, J. Pang, S. M. Bawaked, M. Mokhtar, S. A. Al-Thabaiti and M. Hong, Stepwise Construction of Extra-Large Heterometallic Calixarene-Based Cages, *Inorg. Chem.*, 2015, **54**, 3183–3188; (*g*) D. M. Wood, W. Meng, T. K. Ronson, A. R. Stefankiewicz, J. J. M. Sanders and J. R. Nitschke, Guest-Induced Transformation of a Porphyrin-Edged $Fe^{II}{}_4L_6$ Capsule into a $Cu^{I}Fe^{II}{}_2L_4$ Fullerene Receptor, *Angew. Chem., Int. Ed.*, 2015, **54**, 3988–3992; (*h*) S. J. Lee, S.-H. Cho, K. L. Mulfort, D. M. Tiede, J. T. Hupp and S. T. Nguyen, Cavity-Tailored, Self-Sorting Supramolecular Catalytic Boxes for Selective Oxidation, *J. Am. Chem. Soc.*, 2008, **130**, 16828–16829; (*i*) A. K. Bar, R. Chakrabarty, G. Mostafa and P. S. Mukherjee, Self-Assembly of a Nanoscopic $Pt_{12}Fe_{12}$ Heterometallic Open Molecular Box Containing Six Porphyrin Walls, *Angew. Chem., Int. Ed.*, 2008, **47**, 8455–8459.

6 N. Eren, F. Fadaei-Tirani, R. Scopelliti and K. Severin, Molecular imine cages with π-basic Au_3(pyrazolate) faces, *Chem. Sci.*, 2024, **15**, 3539–3544.

7 For review articles, see: (*a*) J. Zheng, Z. Lu, K. Wu, G.-H. Ning and D. Li, Coinage-Metal-Based Cyclic Trinuclear Complexes with Metal–Metal Interactions: Theories to Experiments and Structures, *Chem. Rev.*, 2020, **120**, 9675–9742; (*b*) J. Zheng, H. Yang, M. Xie and D. Li, The π-acidity/basicity of cyclic trinuclear units (CTUs): from a theoretical perspective to potential applications, *Chem. Commun.*, 2019, **55**, 7134–7146; (*c*) M. A. Omray, A. A. Mohamed, M. A. Rawashdeh-Omary and J. P. Fackler, Jr., Photophysics of supramolecular binary stacks consisting of electron-rich trinuclear Au(I) complexes and organic electrophiles, *Coord. Chem. Rev.*, 2005, **249**, 1372–1381; (*d*) A. Burini, A. A. Mohamed and J. P. Fackler, Cyclic Trinuclear Au(I) Compounds: Synthesis, Structures, and Supramolecuar Acid-Base π-Stacks, *Comments Inorg. Chem.*, 2003, **24**, 253–280.

8 For Au_3(pyrazolate)$_3$-based cages with low solubility, see: (*a*) M. Veronelli, S. Dechert, A. Schober, S. Demeshko and F. Meyer, 1,1′-Bis(pyrazol-4-yl)ferrocenes: Potential Clip Ligands and Their Supramolecular Structures, *Eur. J. Inorg. Chem.*, 2017, 446–453; (*b*) M. Veronelli, S. Dechert, S. Demeshko and F. Meyer, 1,1′-Bis(pyrazol-3-yl)ferrocene: A Clip Ligand That Forms Supramolecular Aggregates and Prismatic Hexanuclear Coinage Metal Complexes, *Inorg. Chem.*, 2015, **54**, 6917–6927; (*c*) T. Jozak, Y. Sun, Y. Schmitt, S. Lebedkin, M. Kappes, M. Gerhards and W. R. Thiel, New Hexanuclear Group 11 Pyrazolate Complexes: Synthesis and Photophysical Features, *Chem. – Eur. J.*, 2011, **17**, 3384–3389.

9 Y. Voloshin, I. Belaya and R. Krämer, *Cage Metal Complexes – Clathrochelates Revisited*, Springer International Publishing, United States, 2017.

10 (*a*) S. Sudan, R.-J. Li, S. M. Jansze, A. Platzek, R. Rudolf, G. H. Clever, F. Fadaei-Tirani, R. Scopelliti and K. Severin, Identification of a Heteroleptic $Pd_6L_6L'_6$ Coordination Cage by Screening of a Virtual Combinatorial Library, *J. Am. Chem. Soc.*, 2021, **143**, 1773–1778; (*b*) O. M. Planes, S. M. Jansze, R. Scopelliti, F. Fadaei-Tirani and K. Severin, Two-Step Synthesis of Linear and Bent Dicarboxylic Acid Metalloligands with Lengths of up to 3 nm, *Inorg. Chem.*, 2020, **59**, 14544–14548; (*c*) G. Cecot, M. T. Doll, O. M. Planes, A. Ramorini, R. Scopelliti, F. Fadaei-Tirani and K. Severin, Cages vs. Prisms: Controlling the Formation of Metallosupramolecular Architectures with Ligand Side-Chains, *Eur. J. Inorg. Chem.*, 2019, 2972–2976; (*d*) S. M. Jansze, D. Ortiz, F. Fadaei Tirani, R. Scopelliti, L. Menin and K. Severin, Inflating face-capped Pd_6L_8 coordination cages, *Chem. Commun.*, 2018, **54**, 9529–9532; (*e*) G. Cecot, M. Marmier, S. Geremia, R. De Zorzi, A. V. Vologzhanina, P. Pattison, E. Solari, F. Fadaei Tirani, R. Scopelliti and K. Severin, The Intricate Structural Chemistry of $M^{II}{}_{2n}L_n$-Type Assemblies, *J. Am. Chem. Soc.*, 2017, **139**, 8371–8381; (*f*) S. M. Jansze, M. D. Wise,

 This journal is © the Partner Organisations 2024

Open Access Article. Published on 29 April 2024. Downloaded on 1/30/2026 12:38:18 AM. This article is licensed under a Creative Commons Attribution 3.0 Unported Licence.

A. V. Vologzhanina, R. Scopelliti and K. Severin, $Pd^{II}_2L_4$-type coordination cages up to three nanometers in size, *Chem. Sci.*, 2017, **8**, 1901–1908; (*g*) G. Cecot, B. Alameddine, S. Prior, R. D. Zorzi, S. Geremia, R. Scopelliti, F. T. Fadaei, E. Solari and K. Severin, Large heterometallic coordination cages with gyrobifastigium-like geometry, *Chem. Commun.*, 2016, **52**, 11243–11246; (*h*) M. D. Wise, J. J. Holstein, P. Pattison, C. Besnard, E. Solari, R. Scopelliti, G. Bricogne and K. Severin, Large, heterometallic coordination cages based on ditopic metallo-ligands with 3-pyridyl donor groups, *Chem. Sci.*, 2015, **6**, 1004–1010.

11 T. Osuga, T. Murase, M. Hoshinoi and M. Fujita, A Tray-Shaped, Pd^{II}-Clipped Au_3 Complex as a Scaffold for the Modular Assembly of [3×*n*] Au Ion Clusters, *Angew. Chem., Int. Ed.*, 2014, **53**, 11186–11189.

12 For examples of tetranuclear Au_4(pyrazolate)$_4$ complexes, see: (*a*) R. A. Smith, R. Kulmaczewski and M. A. Halcrow, Ligand-Directed Metalation of a Gold Pyrazolate Cluster, *Inorg. Chem.*, 2023, **62**, 9300–9305; (*b*) K. Fujisawa, Y. Ishikawa, Y. Miyashita and K.-i. Okamoto, Pyrazolate-bridged group 11 metal(I) complexes: Substituent effects on the supramolecular structures and physicochemical properties, *Inorg. Chim. Acta*, 2010, **363**, 2977–2989; (*c*) G. Yang and R. G. Raptis, Synthesis, structure and properties of tetrameric gold(I) 3,5-di-*tert*-butyl-pyrazolate, *Inorg. Chim. Acta*, 2003, **352**, 98–104.

13 For heterometallic Au/Ag or Au/Cu trimers with different bridging ligands, see: (*a*) R. Galassi, M. M. Ghimire, B. M. Otten, S. Ricci, R. N. McDougald, Jr., R. M. Almotawa, D. Alhmoud, J. F. Ivy, A.-M. M. Rawashdeh, V. N. Nesterov, E. W. Reinheimer, L. M. Daniels, A. Burini and M. A. Omary, Cupriphication of gold to sensitize d^{10}–d^{10} metal–metal bonds and near-unity phosphorescence quantum yields, *Proc. Natl. Acad. Sci. U. S. A.*, 2017, **114**, E5042–E5051; (*b*) A. A. Mohamed, R. Galassi, F. Papa, A. Burini and J. P. Fackler, Jr., Gold(I) and Silver(I) Mixed-Metal Trinuclear Complexes: Dimeric Products from the Reaction of Gold(I) Carbeniates or Benzylimidazolates with Silver(I) 3,5-Diphenylpyrazolate, *Inorg. Chem.*, 2006, **45**, 7770–7776; (*c*) A. A. Mohamed, R. Galassi, A. Burini and J. P. Fackler, Jr., Mixed-Metal Triangular Trinuclear Complexes: Dimers of Gold-Silver Mixed-Metal Complexes from Gold(I) Carbeniates and Silver(I) 3,5-Diphenylpyrazolates, *J. Am. Chem. Soc.*, 2005, **127**, 5012–5013.

14 (*a*) Y.-H. Huang, Y.-L. Lu, X.-D. Zhang, C.-H. Liu, J. Ruan, Y.-H. Qin, Z.-M. Cao, J. Jiang, H.-S. Xu and C.-Y. Su, Dynamic Stereochemistry of M_8Pd_6 Supramolecular Cages Based on Metal-Center Lability for Differential Chiral Induction, Resolution and Recognition, *Angew. Chem., Int. Ed.*, 2024, **63**, e202315053; (*b*) Y.-J. Hou, K. Wu, Z.-W. Wei, K. Li, Y.-L. Lu, C.-Y. Zhu, J.-S. Wang, M. Pan, J.-J. Jiang, G.-Q. Li and C.-Y. Su, Design and Enantioresolution of Homochiral Fe(II)–Pd(II) Coordination Cages from Stereolabile Metalloligands: Stereochemical Stability and Enantioselective Separation, *J. Am. Chem. Soc.*, 2018, **140**, 18183–18191; (*c*) T. Y. Kim, L. Digal, M. G. Gardiner, N. T. Lucas and J. D. Crowley, Octahedral $[Pd_6L_8]^{12+}$ Metallosupramolecular Cages: Synthesis, Structures and Guest-Encapsulation Studies, *Chem. – Eur. J.*, 2017, **23**, 15089–15097; (*d*) K. Wu, K. Li, Y.-J. Hou, M. Pan, L.-Y. Zhang, L. Chen and C.-Y. Su, Homochiral D_4-symmetric metal–organic cages from stereogenic Ru(II) metalloligands for effective enantioseparation of atropisomeric molecules, *Nat. Commun.*, 2016, **7**, 10487; (*e*) T. H. Noh, W. Hong, H. Lee and O.-S. Jung, Indistinguishability and distinguishability between amide and ester moieties in the construction and properties of M_6L_8 octahedral nanocages, *Dalton Trans.*, 2015, **44**, 787–794; (*f*) X.-J. Li, F.-L. Jiang, M.-Y. Wu, S.-Q. Zhang, Y.-F. Zhou and M.-C. Hong, Self-Assembly of Discrete M_6L_8 Coordination Cages Based on a Conformationally Flexible Tripodal Phosphoric Triamide Ligand, *Inorg. Chem.*, 2012, **51**, 4116–4122; (*g*) D. Moon, S. Kang, J. Park, K. Lee, R. P. John, H. Won, G. H. Seong, Y. S. Kim, G. H. Kim, H. Rhee and M. S. Lah, Face-Driven Corner-Linked Octahedral Nanocages: M_6L_8 Cages Formed by C_3-Symmetric Triangular Facial Ligands Linked via C_4-Symmetric Square Tetratopic Pd^{II} Ions at Truncated Octahedron Corners, *J. Am. Chem. Soc.*, 2006, **128**, 3530–3531.

15 J. Zaia, R. S. Annan and K. Biemann, The Correct Molecular Weight for Myoglobin, a Common Calibrant for Mass Spectrometry, *Rapid Commun. Mass Spectrom.*, 1992, **6**, 32–36.

16 For a review article about large metal-based assemblies, see: A. V. Virovets, E. Peresypkina and M. Scheer, Structural Chemistry of Giant Metal Based Supramolecules, *Chem. Rev.*, 2021, **121**, 14485–14554.

17 S. Ivanova, P. Adamski, E. Köster, L. Schramm, R. Fröhlich and F. Beuerle, Size Determination of Organic Cages by Diffusion NMR Spectroscopy, *Chem. – Eur. J.*, 2024, **30**, e202303318.

18 M. Han, D. M. Engelhard and G. H. Clever, Self-assembled coordination cages based on banana-shaped ligands, *Chem. Soc. Rev.*, 2014, **43**, 1848–1860.